Endogenous Peptide Discovery of the Rat Circadian Clock

A FOCUSED STUDY OF THE SUPRACHIASMATIC NUCLEUS BY ULTRAHIGH PERFORMANCE TANDEM MASS SPECTROMETRY*[S]

Ji Eun Lee‡§, Norman Atkins, Jr.¶, Nathan G. Hatcher‖, Leonid Zamdborg‡§, Martha U. Gillette§¶, Jonathan V. Sweedler‡§¶‖, and Neil L. Kelleher‡§‡‡**

Understanding how a small brain region, the suprachiasmatic nucleus (SCN), can synchronize the body's circadian rhythms is an ongoing research area. This important time-keeping system requires a complex suite of peptide hormones and transmitters that remain incompletely characterized. Here, capillary liquid chromatography and FTMS have been coupled with tailored software for the analysis of endogenous peptides present in the SCN of the rat brain. After *ex vivo* processing of brain slices, peptide extraction, identification, and characterization from tandem FTMS data with <5-ppm mass accuracy produced a hyperconfident list of 102 endogenous peptides, including 33 previously unidentified peptides, and 12 peptides that were post-translationally modified with amidation, phosphorylation, pyroglutamylation, or acetylation. This characterization of endogenous peptides from the SCN will aid in understanding the molecular mechanisms that mediate rhythmic behaviors in mammals. ***Molecular & Cellular Proteomics 9:285–297, 2010.***

Central nervous system neuropeptides function in cell-to-cell signaling and are involved in many physiological processes such as circadian rhythms, pain, hunger, feeding, and body weight regulation (1–4). Neuropeptides are produced from larger protein precursors by the selective action of endopeptidases, which cleave at mono- or dibasic sites and then remove the C-terminal basic residues (1, 2). Some neuropeptides undergo functionally important post-translational modifications (PTMs),[1] including amidation, phosphorylation, pyroglutamylation, or acetylation. These aspects of peptide synthesis impact the properties of neuropeptides, further expanding their diverse physiological implications. Therefore, unveiling new peptides and unreported peptide properties is critical to advancing our understanding of nervous system function.

Historically, the analysis of neuropeptides was performed by Edman degradation in which the N-terminal amino acid is sequentially removed. However, analysis by this method is slow and does not allow for sequencing of the peptides containing N-terminal PTMs (5). Immunological techniques, such as radioimmunoassay and immunohistochemistry, are used for measuring relative peptide levels and spatial localization, but these methods only detect peptide sequences with known structure (6). More direct, high throughput methods of analyzing brain regions can be used.

Mass spectrometry, a rapid and sensitive method that has been used for the analysis of complex biological samples, can detect and identify the precise forms of neuropeptides without prior knowledge of peptide identity, with these approaches making up the field of peptidomics (7–12). The direct tissue and single neuron analysis by MALDI MS has enabled the discovery of hundreds of neuropeptides in the last decade, and the neuronal homogenate analysis by fractionation and subsequent ESI or MALDI MS has yielded an equivalent number of new brain peptides (5). Several recent peptidome studies, including the work by Dowell *et al.* (10), have used the specificity of FTMS for peptide discovery (10, 13–15). Here, we combine the ability to fragment ions at ultrahigh mass accuracy (16) with a software pipeline designed for neuropeptide discovery. We use nanocapillary reversed-phase LC coupled to 12 Tesla FTMS for the analysis of peptides present in the suprachiasmatic nucleus (SCN) of rat brain.

A relatively small, paired brain nucleus located at the base of the hypothalamus directly above the optic chiasm, the SCN contains a biological clock that generates circadian rhythms in behaviors and homeostatic functions (17, 18). The SCN comprises ~10,000 cellular clocks that are integrated as a tissue level clock which, in turn, orchestrates circadian rhythms throughout the brain and body. It is sensitive to incoming signals from the light-sensing retina and other brain regions, which cause temporal adjustments that align the

From the Departments of ‡Chemistry and **Cell and Developmental Biology, §Institute for Genomic Biology, ¶Neuroscience Program, and ‖Beckman Institute, University of Illinois at Urbana-Champaign, Urbana, Illinois 61801

Received, August 6, 2009, and in revised form, November 3, 2009
Published, MCP Papers in Press, November 10, 2009, DOI 10.1074/mcp.M900362-MCP200

[1] The abbreviations used are: PTM, post-translational modification; SCN, suprachiasmatic nucleus; ZT, Zeitgeber time; .puf, ProSight upload file; GRP, gastrin-releasing peptide; VIP, vasoactive intestinal peptide; PACAP, pituitary adenylate cyclase-activating polypeptide; AVP, arginine-vasopressin; GABA, γ-aminobutyric acid; CART, cocaine- and amphetamine-regulated transcript protein; DRP, dihydropyrimidinase-related protein; LTQ, linear trap quadrupole; AA, amino acids.

© 2010 by The American Society for Biochemistry and Molecular Biology, Inc.
This paper is available on line at http://www.mcponline.org

SCN appropriately with changes in environmental or behavioral state. Previous physiological studies have implicated peptides as critical synchronizers of normal SCN function as well as mediators of SCN inputs, internal signal processing, and outputs; however, only a small number of peptides have been identified and explored in the SCN, leaving unresolved many circadian mechanisms that may involve peptide function.

Most peptide expression in the SCN has only been studied through indirect antibody-based techniques (19–29), although we recently used MS approaches to characterize several peptides detected in SCN releasates (30). Previous studies indicate that the SCN expresses a rich diversity of peptides relative to other brain regions studied with the same techniques. Previously used immunohistochemical approaches are not only inadequate for comprehensively evaluating PTMs and alternate isoforms of known peptides but are also incapable of exhaustively examining the full peptide complement of this complex biological network of peptidergic inputs and intrinsic components. A comprehensive study of SCN peptidomics is required that utilizes high resolution strategies for directly analyzing the peptide content of the neuronal networks comprising the SCN.

In our study, the SCN was obtained from *ex vivo* coronal brain slices via tissue punch and subjected to multistage peptide extraction. The SCN tissue extract was analyzed by FTMS/MS, and the high resolution MS and MS/MS data were processed using ProSightPC 2.0 (16), which allows the identification and characterization of peptides or proteins from high mass accuracy MS/MS data. In addition, the Sequence Gazer included in ProSightPC was used for manually determining PTMs (31, 32). As a result, a total of 102 endogenous peptides were identified, including 33 that were previously unidentified, and 12 PTMs (including amidation, phosphorylation, pyroglutamylation, and acetylation) were found. The present study is the first comprehensive peptidomics study for identifying peptides present within the mammalian SCN. In fact, this is one of the first peptidome studies to work with discrete brain nuclei as opposed to larger brain structures and follows up on our recent report using LC-ion trap for analysis of the peptides in the supraoptic nucleus (33); here, the use of FTMS allows a greater range of PTMs to be confirmed and allows higher confidence in the peptide assignments. This information on the peptides in the SCN will serve as a basis to more exhaustively explore the extent that previously unreported SCN neuropeptides may function in SCN regulation of mammalian circadian physiology.

EXPERIMENTAL PROCEDURES

Materials—All reagents were obtained from Sigma-Aldrich unless otherwise noted. Siliconized microcentrifuge tubes (1.5 ml) were purchased from Thermo Fisher Scientific (San Jose, CA). Microcon YM-10 centrifugal filter devices were purchased from Millipore (Billerica, MA).

Animals and Circadian Time—An inbred strain of 8–10-week-old female Long-Evans rats, LE-BluGill, demonstrated to be genetically homogeneous by high density genome scan (34) was used for these studies. Animals were fed *ad libitum* and were housed under constant temperature and humidity conditions in a 12:12 h light/dark cycle environment. Animals were entrained to this lighting schedule for at least 10 days prior to tissue collection. All collections of *ex vivo* SCN tissue samples were conducted during mid-subjective daytime ~6–7 h following onset of normal lights-on conditions, referred to as Zeitgeber time (ZT) 6–7. All vertebrate animal procedures were carried out with protocols approved by the University of Illinois at Urbana-Champaign Institutional Animal Care and Use Committee and in full compliance with National Institutes of Health guidelines for humane animal care.

Preparation of SCN Brain Punch Samples—Animal subjects were decapitated, and the brain was immediately removed from the skull. The hypothalamus was blocked, and using a mechanical tissue chopper, coronal brain sections (500-μm thickness) were prepared. A brain section containing the mid-SCN was retained. A 2-mm-diameter sample corer was used to excise the paired SCN from the surrounding hypothalamus, aligning the top edge of the corer with the dorsal SCN border (see supplemental Fig. S1). This punch technique results in minimal harvest of extra-SCN hypothalamic tissue. Optic nerve tissue at the level of the optic chiasm is contained within the SCN-containing punch. Peptidome analysis of rat optic nerve tissue produces a peptidomic profile distinct from our SCN peptidomics data (unpublished data). The SCN punch preparation was performed in glucose-/bicarbonate-/gentamicin-supplemented Earle's balanced salt solution (Invitrogen) perfused with 95% O_2, 5% CO_2. SCN-containing punches were immediately transferred to a siliconized microcentrifuge tube that remained submerged in powered dry ice until the time of peptide extraction.

Peptide Extraction from SCN Punches—Either 12 or 24 SCN punches were pooled and subjected to multistage peptide extraction as described in the recent work by Bora *et al.* (33). First, 150 or 300 μl of deionized water, preheated to 90 °C, was added to the SCN punches. The sample was boiled for 10 min and centrifuged at 14,000 $\times$ *g* for 10 min. The resulting tissue pellet was subjected to the second stage of extraction, whereas the supernatant was retained in a new microcentrifuge tube. After addition of 150 or 300 μl of ice-cold acidified acetone (40:6:1 acetone/water/HCl), the sample was homogenized with ultrasonic cleaner FS30 (Thermo Fisher Scientific) for 30 s, vortexed for 1 min, and kept on ice for 1 h. The sample was vortexed again for 1 min and centrifuged at 14,000 $\times$ *g* for 20 min at 4 °C, and the supernatant was saved. Then, a third extraction was performed by adding 150 or 300 μl of ice-cold 0.25% acetic acid to the tissue pellet and incubating on ice for 1 h. The acidified acetone extract was neutralized by 1 M NaOH and dried to 10–20 μl to remove the acetone. All of the extracts were combined and filtered through a Microcon centrifugal filter device (10-kDa-molecular mass cutoff). Finally, the filtered extract was concentrated using a SpeedVac and used for nanocapillary FTMS/MS injection.

Mass Spectral Analysis (LC-FTMS/MS)—The extracted peptides from the SCN punches were analyzed using a 12 Tesla LTQ-FT Ultra (Thermo Fisher Scientific) interfaced with a 1D NanoLC pump from Eksigent Technologies (Dublin, CA). The sample was loaded with helium bomb pressure (500 p.s.i.) to a trap column (75-μm inner diameter), 5 cm of which was fritted with LiChrosorb (EM Separations, Gibbstown, NJ) and packed with a C_{18} solid phase (10 μm; YMC Co., Ltd., Allentown, PA). The analytical column used ProteoPep™ II medium (C_{18}, 300 Å, 5 μm) and was purchased from New Objective (Woburn, MA). The operating flow rate was 300 nl/min with the following gradient conditions: 0–20 min, 0–15% B; 20–90 min, 15–35% B; 90–180 min, 35–60% B; 180–220 min, 60–80% B; 220–240 min, 80–100% B; 240–250 min, 100–0% B; and 250–260 min, 0–5% B. Data acquisition on the LTQ-FTMS instrument consisted of a full scan

event (290–2000 *m/z*; resolving power, $m/\Delta m_{50\%}$ = 90,000 in which $\Delta m_{50\%}$ is the mass spectral peak full width at half-maximum peak height) and data-dependent CID MS/MS scans (40,000 resolving power) of the five most abundant peaks from the previous full scan. MS/MS settings were as follows: isolation width, *m/z* 5; minimum signal threshold, 1000 counts; normalized collision energy, 35%; activation Q, 0.4; and activation time, 50 ms. Dynamic exclusion was enabled with a repeat count of 4, an exclusion duration of 180 s, and a repeat duration of 30 s.

Data Analysis—Resulting LC-FTMS/MS files (*.raw) were analyzed using ProSightPC 2.0 (Thermo Fisher Scientific) (16), which has several software component algorithms including cRAWler 2.0, which interprets resolved isotopic distributions based on the Xtract or thorough high resolution analysis of spectra by Horn (THRASH) algorithms. The cRAWler program first determines all precursor mass values according to user-specified tolerances such as ranges of *m/z* and retention time or signal-to-noise ratio and fitting parameters. The precursor and fragmentation scans corresponding to these precursors are then separately averaged and interpreted to provide a list of monoisotopic masses. This information is compiled into a ProSight upload file (.puf). In multiplexing mode, cRAWler can capture multiple precursor masses within the isolation range as multiple precursors based on an intensity cutoff (set at 10% here) relative to the base peak of the analysis window. This allows for cases where multiple precursors are fragmented together (see below).

Database Searching—Each .puf file, which typically contained hundreds of experiments from a single nano-LC-MS/MS run, was first searched in absolute mass mode (MS1 and MS2 tolerances of ±10 ppm) against a database of predicted rat neuropeptides (with and without predicted modifications) generated by taking the set of known rat prohormones processed *in silico* via the NeuroPred algorithm (35–37). For the searches that did not identify a peptide below an E-value cutoff of 10^{-4}, a search in "neuropeptide" mode was initiated against an intact rat database (UniProt 15.0, 4,318,021 protein forms) with ±100-Da intact mass and ±10-ppm fragment tolerance. Neuropeptide mode scans across sequences to find candidate subsequences whose masses are within tolerance of a precursor mass (no protease specificity); experimental fragment masses are then matched with theoretical fragment masses from these candidate subsequences. Neuropeptide searches along with the other mode described in this work are available through neuroProSight over the internet. A Sequence Gazer tool in neuroProSight software was used for manually determining PTMs on the peptides. The peptides identified from multiplexing mode were manually validated.

RESULTS

Two-millimeter-diameter punches of ventral hypothalamic tissue (500-μm thickness) containing the bilaterally paired SCN were excised from rat coronal brain slices. At least six SCN punches, which contained ~360 μg of total protein amount based on BCA assay, were needed for a high content nanocapillary FTMS/MS run. From a total of 10 LC-MS/MS runs for the SCN peptidome analysis, 102 endogenous peptides derived from 27 precursor proteins were identified along with 12 PTMs (amidation, phosphorylation, pyroglutamylation, and acetylation) (see Table 1). The average E-value for identification was 4×10^{-21}, 17 orders of magnitude below the conservative threshold of 10^{-4} used here. This remarkable certainty of identification arises from the use of fragmentation scans with high mass accuracy and a scoring/software system that converts these data into peptide identifications with high fidelity. Thirty-three peptides (Table I, denoted with Footnote c) were not previously identified in either mouse or rat brain studies. The references for the identified peptides found in the prior studies of brain as well as SCN are included in a column of Table I. For example, the peptides derived from the prohormones gastrin-releasing peptide (GRP) and vasoactive intestinal peptide (VIP) are intrinsic SCN peptides that have received considerable attention (17, 22, 23, 25, 28, 38–55). Surprisingly, peptides from 12 precursor proteins found in our SCN peptidome study, including cocaine- and amphetamine-regulated transcript protein (CART), cerebellin-1, and proenkephalin B, were not reported in prior SCN studies. Finally, information from mRNA expression data from the mouse SCN reported in the Allen Brain Atlas (56) is included in Table I and highlights localization of prohormone synthesis for the prohormones identified from our present study. In addition to the endogenous peptides derived from prohormones, 66 peptide fragments from proteins like hemoglobin subunit β-1 and myelin basic protein S were also identified (supplemental Table 1). Although peptides that are protein fragments could result from post-mortem degradation during sample preparation, they may be the products of prohormone processing that are physiologically relevant. For example, small peptides formed from hemoglobin, the hemopressins, have known bioactivity and are likely enzymatically produced and are not formed during post-mortem degradation (57–59).

Fig. 1 depicts the examples of FTMS and MS/MS spectra for prohormone-derived peptide forms of VIP and pituitary adenylate cyclase-activating polypeptide (PACAP) identified with E-values of 9×10^{-16} and 2×10^{-27}, respectively. Although the sequence of VIP is HSDAVFTDNYTRLRKQMAVKKYLNSI (AA 125–152), another peptide from the VIP prohormone was identified in this study: HSDAVFTDNYTRL (AA 125–137). Because the observed peptide sequence results from cleavage of the prohormone at a dibasic cleavage site (RK), it appears to be a *bona fide* intracellular processing product from the VIP prohormone and is not expected to arise from extracellular degradation/processing. This shortened peptide has been reported in SwePep. The observed peptide derived from the PACAP prohormone was GMGENLAAAAVDDRAPLT (AA 111–128), whereas the previously confirmed bioactive PACAP-derived peptides are PACAP-27 (AA 131–157) and PACAP-38 (AA 131–168). Because there are dibasic residues (KR) between the observed peptide and the PACAP-27 and -38, again we assume that the observed peptide was produced from the intracellular processing of the PACAP prohormone.

Fig. 2 represents the FTMS and MS/MS spectra for cerebellin (AA 57–72) and a one-amino acid-truncated form (AA 57–71), which are derived from the cerebellin-1 precursor. The two peptides co-eluted, as seen in Fig. 2*A*, and were identified by the data-dependent top five MS/MS acquisition strategy as seen in Fig. 2*B*. These two cerebellin forms were previously identified from mouse hypothalamus studies (8); however,

TABLE I

Peptides identified from SCN peptidome analysis

PTMs are shown in bold. NPY, neuropeptide Y; MCH, melanin-concentrating hormone; POMC, proopiomelanocortin.

Precursor	Peptide name	Sequence	Observed mass	Mass difference	E-value[a]	UniProt accession number	Refs. of brain studies	Refs. of SCN studies[b]	Allen Brain Atlas mRNA expression data
			Da	*ppm*					
CART (AA 37–55)		ALDIYSAVDDASHEKELPR	2128.05	4.1	4×10^{-18}	P49192	12		mouse.brain-map.org/brain/gene/72077479.html?ispopup=1
CART (AA 60–77)		APGAVLQIEALQEVLKKL	1919.15	3.6	6×10^{-6}	P49192	102		
CART (AA 60–79)		APGAVLQIEALQEVLKKLKS	2134.28	3.4	6×10^{-29}	P49192	102		
Cerebellin-1 (AA 57–71)		SGSAKVAFSAIRSTN	1494.78	0.6	1×10^{-10}	P63182	8		
Cerebellin-1 (AA 57–72)	Cerebellin	SGSAKVAFSAIRSTNH	1631.84	2.3	7×10^{-17}	P63182	8		
GRP (AA 24–41)		APVSTGAGGGTVLAKMYP	1675.87	4.6	6×10^{-7}	P24393	SwePep	17, 22, 23, 25, 38–47	mouse.brain-map.org/brain/gene/1363.html?ispopup=1
Pro-MCH (AA 32–55)[c]		NVEDDIVFNTFRMGKAFQKEDTAE	2803.32	−1.3	4×10^{-10}	P14200		103	
Pro-MCH (AA 131–143)	Neuropeptide-glutamic acid-isoleucine	EIGDEENSAKFP**I(amidation)**	1446.70	2.8	5×10^{-35}	P14200	63		
Neuropeptide Y (AA 69–97)[c]		SSPETLISDLLMRESTENAPRTRLEDPSM	3274.59	6.9	7×10^{-7}	P07808		77–86, 88–91	mouse.brain-map.org/brain/gene/717.html?ispopup=1
Neuropeptide Y (AA 69–98)	C-flanking peptide of NPY (CPON)	SSPETLISDLLMRESTENAPRTRLEDPSMW	3460.67	8.2	3×10^{-13}	P07808	8		
Neurosecretory protein VGF (AA 24–60)		APPGRSDVYPPPLGSEHNGQVAEDAVSR PKDDSVPEV	3867.88	4.5	3×10^{-21}	P20156	104	24, 105–108	mouse.brain-map.org/brain/gene/71924165.html?ispopup=1
Neurosecretory protein VGF (AA 24–63)		APPGRSDVYPPPLGSEHNGQVAEDAVS RPKDDSVPEVRAA	4166.06	3.5	1×10^{-13}	P20156	104		
Neurosecretory protein VGF (AA 238–282)[c]		MSENVPLPETHQFGEGVSSPKTHLGETL TPLSKAYQSLSAPFPKV	4835.45	7.9	2×10^{-15}	P20156			
Neurosecretory protein VGF (AA 285–309)		LEGSFLGGSEAGERLLQQGLAQVE**A(amidation)**	2557.32	1.0	1×10^{-21}	P20156	109		
Neurosecretory protein VGF (AA 487–507)		KKNAPPEPVPPPRAAPAPTHV	2170.21	3.6	3×10^{-3}	P20156	102		
Neurosecretory protein VGF (AA 489–507)		NAPPEPVPPPRAAPAPTHV	1914.02	3.0	7×10^{-18}	P20156	102		
Neurosecretory protein VGF (AA 601–617)		EQEELENYIEHVLLHRP	2147.08	5.6	6×10^{-6}	P20156	104		
Neuroendocrine protein 7B2 (AA 25–49)[c]		YSPRTP DRVSETDIQR LLHGVMEQL	2939.51	5.3	8×10^{-10}	P27682			
PACAP (AA 111–128)		GMGENLAAAAVDDRAPLT	1770.87	5.5	2×10^{-27}	P13589	10, 63	64–66, 68–76, 110	mouse.brain-map.org/brain/gene/74511882.html?ispopup=1
POMC (AA 124–136)	Melanotropin α	SYSMEHFRWGKP**V(amidation)**	1621.79	3.0	2×10^{-27}	Q8K422	8, 30, 61, 111	17, 112, 113	mouse.brain-map.org/brain/gene/80517122.html?ispopup=1
POMC (AA 141–158)		RPVKVYPNVAENESAEAF	2505.26	4.6	3×10^{-7}	Q8K422	8, 61		
POMC (AA 165–202)	Lipotropin gamma	ELEGEQPDGLEHVLEPDTEKADGPY RVEHFRWGNPPKD	4385.09	6.4	9×10^{-10}	Q8K422	12, 61		
POMC (AA 205–235)	Beta-endorphin	YGGFMTSEKSQTPLVTLFKNAIIKNAHKKGQ	3435.85	4.4	6×10^{-7}	Q8K422	102		
Proenkephalin A (AA 114–133)		MDELYPVEPEEEANGGEILA	2204.00	5.4	5×10^{-8}	P04094	33	114, 115	mouse.brain-map.org/brain/gene/74881286.html?ispopup=1
Proenkephalin A (AA 143–185)		DADEGDTLANSSDLLKELLGTGDNRAKDSHQ QESTNNDEDSTS	4592.04	−2.8	2×10^{-34}	P04094	116		
Proenkephalin A (AA 188–195)	Met-enkephalin-Arg-Gly-Leu	YGGFMRGL	899.44	3.5	4×10^{-18}	P04094	63		
Proenkephalin A (AA 198–209)		SPQLEDEAKELQ	1385.67	2.0	6×10^{-31}	P04094	12, 63		
Proenkephalin A (AA 219–229)		VGRPEWWMDYQ	1465.65	2.6	6×10^{-15}	P04094	12, 33, 63		
Proenkephalin A (AA 239–259)[c]		FAESLPSDEEGE SYSKEVPEM	2359.02	7.1	2×10^{-3}	P04094			
Proenkephalin A (AA 263–269)	Met-enkephalin-Arg-Phe	YGGFMRF	876.40	3.4	5×10^{-22}	P04094	63		
Proenkephalin B (AA 235–248)		SQENPNTYSEDLDV	1609.68	4.2	1×10^{-16}	P06300	33		
Protachykinin 1 (AA 58–68)	Substance P	RPKPQQFFGL**M(amidation)**	1346.73	3.5	9×10^{-19}	P06767	30, 63	29, 117–123	mouse.brain-map.org/brain/gene/1038.html?ispopup=1
Protachykinin 1 (AA 72–94)		DADSSIEKQVALLKALYGHGQIS	2442.29	4.8	4×10^{-9}	P06767	11		

TABLE I—*continued*

Precursor	Peptide name	Sequence	Observed mass	Mass difference	E-value[a]	UniProt accession number	Refs. of brain studies	Refs. of SCN studies[b]	Allen Brain Atlas mRNA expression data
			Da	*ppm*					
Pro-SAAS (AA 34–40)	KEP	ARPVKEP	795.46	−0.6	1×10^{-2}	Q9QXU9	124	30	mouse.brain-map.org/brain/gene/777.html?ispopup=1
Pro-SAAS (AA 34–59)	Big SAAS	ARPVKEPRSLSAASAPLAETSTPLRL	2448.34	3.5	4×10^{-32}	Q9QXU9	8		
Pro-SAAS (AA 42–57)		SLSAASAPLAETSTPL	1514.79	3.3	5×10^{-27}	Q9QXU9	33		
Pro-SAAS (AA 42–59)	Little SAAS	SLSAASAPLAETSTPLRL	1783.98	4.0	4×10^{-41}	Q9QXU9	30, 33		
Pro-SAAS (AA 44–57)		SAASAPLAETSTPL	1314.67	1.2	4×10^{-13}	Q9QXU9	SwePep		
Pro-SAAS (AA 44–59)		SAASAPLAETSTPLRL	1583.86	4.4	2×10^{-28}	Q9QXU9	33		
Pro-SAAS (AA 48–59)		APLAETSTPLRL	1267.72	3.5	4×10^{-32}	Q9QXU9	10		
Pro-SAAS (AA 62–75)		AVPRGEAAGAVQEL	1366.72	4.3	8×10^{-27}	Q9QXU9	10, 33		
Pro-SAAS (AA 62–89)		AVPRGEAAGAVQELARALAHLLEAERQE	2954.57	2.1	8×10^{-50}	Q9QXU9	8		
Pro-SAAS (AA 62–120)[c]		AVPRGEAAGAVQELARALAHLLEA ERQERARAEAQEAEDQQARV LAQLLRAWGSPRASD	6385.36	5.1	1×10^{-14}	Q9QXU9			
Pro-SAAS (AA 62–143)[c]		AVPRGEAAGAVQELARALAHLLEAERQERA RAEAQEAEDQQARVLAQLLRAWGSPR ASDPPLAPDDDPDAPAAQLARALLRA	8720.54	−2.2	1×10^{-23}	Q9QXU9			
Pro-SAAS (AA 113–143)[c]		WGSPRASDPPLAPDDDPDAPAAQLARALLRA	3209.62	−1.0	6×10^{-9}	Q9QXU9			
Pro-SAAS (AA 121–143)[c]		PPLAPDDDPDAPAAQLARALLRA	2353.25	2.3	1×10^{-8}	Q9QXU9			
Pro-SAAS (AA 174–218)[c]		GPTGPDVEDAADETPDVDPELLRYL LGRILTGSSEPEAAPAPRRL	4755.42	3.9	2×10^{-10}	Q9QXU9			
Pro-SAAS (AA 221–239)[c]		AVDQDLGPEVPPENVLGAL	1931.99	2.8	1×10^{-37}	Q9QXU9			
Pro-SAAS (AA 221–240)	PEN-20	AVDQDLGPEVPPENVLGALL	2045.08	0.0	1×10^{-12}	Q9QXU9	8		
Pro-SAAS (AA 221–241)[c]		AVDQDLGPEVPPENVLGALLR	2201.18	3.7	1×10^{-17}	Q9QXU9			
Pro-SAAS (AA 221–242)	PEN	AVDQDLGPEVPPENVLGALLRV	2300.25	3.5	4×10^{-32}	Q9QXU9	30, 33		
Pro-SAAS (AA 245–260)	Big LEN	LENSSPQAPARRLLPP	1744.96	5.3	6×10^{-39}	Q9QXU9	30, 33		
Prothyroliberin (AA 25–50)		LPEAAQEEGAVTPDLPGLENVQVRPE	2757.40	5.0	9×10^{-22}	P01150	8	125, 126	
Prothyroliberin (AA 83–103)[c]		EEEEKDIEAEERGDLGEGGAW	2347.02	4.6	7×10^{-5}	P01150			
Prothyroliberin (AA 178–199)		FIDPELQRSWEEKEGEGVLMPE	2617.25	4.8	1×10^{-20}	P01150	8		
Secretogranin 1 (AA 372–380)		SEESQEKEY	1127.46	1.0	4×10^{-13}	O35314	11		
Secretogranin 1 (AA 416–432)		GRGREPGAYPALDSRQE	1857.91	1.3	2×10^{-9}	O35314	127		
Secretogranin 1 (AA 513–532)		LGALFNPYFDPLQWKNSDFE	2400.14	4.2	2×10^{-35}	O35314	128		
Secretogranin 1 (AA 585–594)		SFAKAPHLDL	1097.59	4.5	4×10^{-17}	O35314	63		
Secretogranin 1 (AA 597–611)		**Q(pyroglutamylation)**YDDGVAELDQLLHY	1760.79	2.8	4×10^{-23}	O35314	97		
Secretogranin 2 (AA 168–181)[c]		FPLMYEENSRENPF	1771.80	4.5	6×10^{-19}	P10362		94	mouse.brain-map.org/brain/gene/934.html?ispopup=1
Secretogranin 2 (AA 169–181)[c]		PLMYEENSRENPF	1624.73	4.5	2×10^{-8}	P10362			
Secretogranin 2 (AA 184–216)	Secretoneurin	TNEIVEEQYTPQSLATLESVFQELGKLTGPSNQ	3649.81	3.2	1×10^{-17}	P10362	102		
Secretogranin 2 (AA 188–216)[c]		ATLESVFQELGKLTGPSNQ	2018.04	5.1	8×10^{-11}	P10362			
Secretogranin 2 (AA 205–216)		QELGKLTGPSNQ	1270.65	2.2	2×10^{-5}	P10362	61		
Secretogranin 2 (AA 287–316)[c]		SGHLGLPDEGNRKESKDQLSEDAS KVITYL	3285.66	4.3	5×10^{-29}	P10362			
Secretogranin 2 (AA 495–517)[c]		PYDNLNDKDQELGEYLARMLVKY	2786.37	4.4	4×10^{-13}	P10362			
Secretogranin 2 (AA 529–566)[c]		VPSPGSSEDDLQEEEQLEQAI KEHLGQGSSQEMEKLAK	4179.99	3.8	2×10^{-20}	P10362			
Secretogranin 2 (AA 529–568)	Manserin	VPSPGSSEDDLQEEEQLEQAIK EHLGQGSSQEMEKLAKVS	4366.09	2.7	6×10^{-50}	P10362	33		
Secretogranin 2 (AA 529–568)[c]	Manserin	VPSPG**S(phosphorylation)** SEDDLQEEE QLEQAIKEHLGQGSSQEMEKLAKVS	4446.06	4.8	4×10^{-23}	P10362			
Secretogranin 2 (AA 571–583)		IPAGSLKNEDTPN	1354.67	1.6	5×10^{-46}	P10362	11		
Secretogranin 2 (AA 571–584)[c]		IPAGSLKNEDTPNR	1510.78	3.1	1×10^{-30}	P10362			
Secretogranin 2 (AA 571–585)[c]		IPAGSLKNEDTPNRQ	1638.84	2.5	2×10^{-28}	P10362			

TABLE I—*continued*

Precursor	Peptide name	Sequence	Observed mass	Mass difference	E-value[a]	UniProt accession number	Refs. of brain studies	Refs. of SCN studies[b]	Allen Brain Atlas mRNA expression data
			Da	*ppm*					
Secretogranin 2 (AA 571–611)[c]		IPAGSLKNEDTPNRQYLDEDMLLK VLEYLNQEQAEQGREHL	4796.38	3.0	1×10^{-71}	P10362			
Secretogranin 2 (AA 571–612)[c]		IPAGSLKNEDTPNRQYLDEDMLL KVLEYLNQEQAEQGREHLA	4867.43	1.4	2×10^{-76}	P10362			
Secretogranin 2 (AA 595–611)[c]		VLEYLNQEQAEQGREHL	2055.01	2.6	5×10^{-24}	P10362			
Secretogranin 3 (AA 23–36)		FPKPEGSQDKSLHN	1582.78	2.4	3×10^{-14}	P47868	33		mouse.brain-map.org/brain/gene/73718057.html?ispopup=1
Somatostatin (AA 25–87)[c]		APSDPRLRQFLQKSLAAATGKQEL AKYFLAELLSEPNQTENDALE PEDLPQAAEQDEMRLELQ	7093.62	7.4	6×10^{-10}	P60042		17, 20, 27, 129–131	mouse.brain-map.org/brain/gene/1001.html?ispopup=1
Tachykinin 3 (AA 95–115)[c]		NSQPDT PADVVEENTPSFGVL	2215.04	4.4	9×10^{-40}	P08435			
Provasopressin (AA 24–32)	Arginine-vasopressin	C[d]YFQNC[d]PR**G(amidation)**	1083.44	0.0	8×10^{-10}	P01186	30, 33, 61	132	mouse.brain-map.org/brain/gene/131.html?ispopup=1
Provasopressin (AA 26–32)[c]		FQNCPR**G(amidation)**	819.38	1.6	4×10^{-16}	P01186			
Provasopressin (AA 151–165)		VQLAGTQESVDSAKP	1528.77	−1.3	3×10^{-17}	P01186	102		
Provasopressin (AA 151–166)		VQLAGTQESVDSAKPR	1684.88	1.3	1×10^{-27}	P01186	133		
Provasopressin (AA 151–167)		VQLAGTQESVDSAKPRV	1783.95	4.2	6×10^{-27}	P01186	SwePep		
Provasopressin (AA 151–168)		VQLAGTQESVDSAKPRVY	1947.01	1.8	5×10^{-38}	P01186	33, 63, 102		
Provasopressin (AA 152–168)[c]		QLAGTQESVDSAKPRVY	1847.94	3.4	8×10^{-20}	P01186			
Provasopressin (AA 153–168)		LAGTQESVDSAKPRVY	1719.88	2.3	9×10^{-32}	P01186	SwePep		
Provasopressin (AA 154–168)		AGTQESVDSAKPRVY	1606.80	0.5	2×10^{-31}	P01186	33		
Provasopressin (AA 155–168)		GTQESVDSAKPRVY	1535.76	1.6	4×10^{-23}	P01186	33		
VIP peptides (AA 125–137)		HSDAVFTDNYTRL	1537.72	4.2	1×10^{-15}	P01283	SwePep	25, 28, 48–55	mouse.brain-map.org/brain/gene/77371835.html?ispopup=1
Acyl-CoA-binding protein (AA 2–87)		**S(acetylation)**QADFDKAAEEVKRLKTQPT DEEMLFIYSHFKQATVGDVNTDRPGLL DLKGKAKWDSWNKLKGTSKENAMKTYV EKVEELKKKYGI	9932.13	1.1	3×10^{-43}	P11030	134, 135		
Brain-specific polypeptide PEP-19 (AA 2–62)		**S(acetylation)**ERQSAGATNG KDKTSGDNDGQKKVQEEFDIDMDAP ETERAAVAIQSQFRKFQKKKAGSQS	6714.25	−1.9	7×10^{-13}	P63055	136		
PEBP-1 (AA 9–25)		AGPLSLQEVDEPPQHAL	1799.92	5.8	3×10^{-22}	P31044	10		
PEBP-1 (AA 11–25)[c]		PLSLQEVDEPPQHAL	1671.85	0.4	3×10^{-18}	P31044			
PEBP-1 (AA 28–46)		DYGGVTVDELGKVLTPTQV	1990.03	2.8	6×10^{-29}	P31044	10		
PEBP-1 (AA 50–66)		PSSISWDGLDPGKLYTL	1847.93	1.6	2×10^{-5}	P31044	137		
PEBP-1 (AA 174–187)		DDSVPKLHDQLAGK	1521.78	3.5	2×10^{-7}	P31044	10		
GABA(A) receptor subunit α-6 (AA 38–55)[c]		NLLEGYDNRLRPGFGGAV	1947.01	8.0	5×10^{-7}	P30191		87	mouse.brain-map.org/brain/gene/75551467.html?ispopup=1
Dihydropyrimidinase-related protein 2 (AA 518–572)[c]		SAKTSPAKQQAPPVRNLHQSGFSLSGAQID DNIPRRTTQRIVAPPGGRANITSLG	5761.09	4.8	3×10^{-48}	P47942			
Dihydropyrimidinase-related protein 2 (AA 560–572)[c]		APPGGRANITSLG	1209.65	1.9	3×10^{-13}	P47942			
Dihydropyrimidinase-related protein 3 (AA 558–570)[c]		APPGGRSNITSLS	1255.65	1.9	6×10^{-12}	Q62952			

[a] E-values above 1×10^{-4} were manually validated.

[b] References found in SCN studies were for the prohormones, which were previously reported in the studies.

[c] Novel peptides.

[d] Cys-Cys bonds.

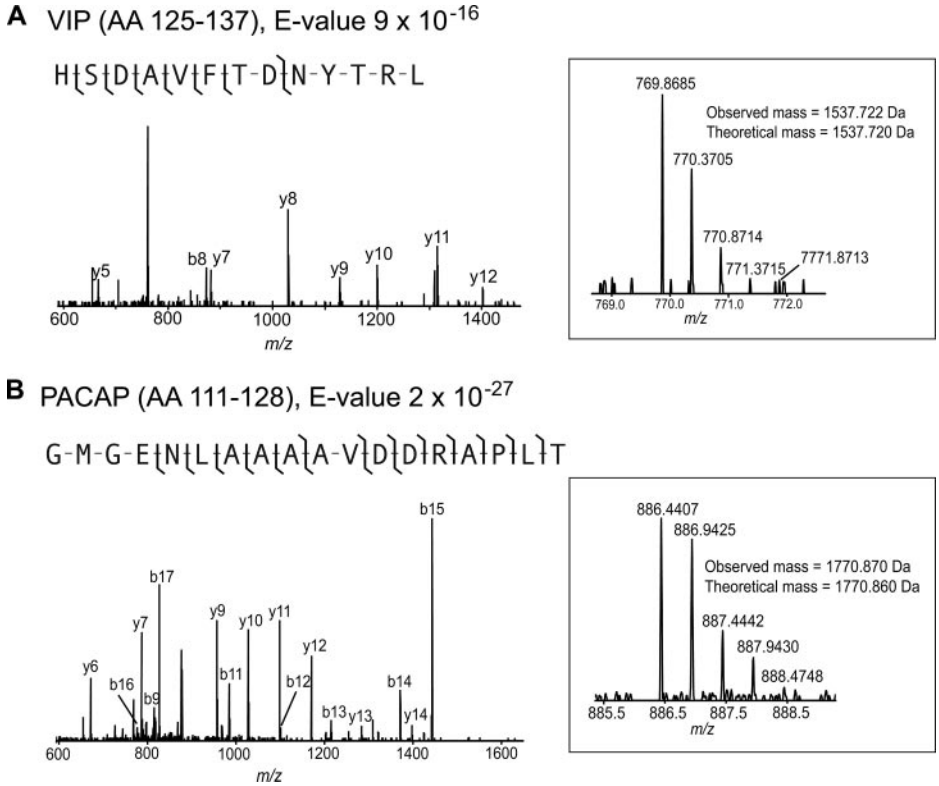

FIG. 1. **FTMS and FTMS/MS data allow identification of peptides present in SCN sample with high confidence.** The peptides derived from VIP (*A*) and PACAP (*B*) were identified with one b-ion and seven y-ions and with eight b-ions and eight y-ions, respectively. VIP is known to be present in SCN core neurons, and PACAP is synthesized within the retinal ganglion cells that innervate the SCN.

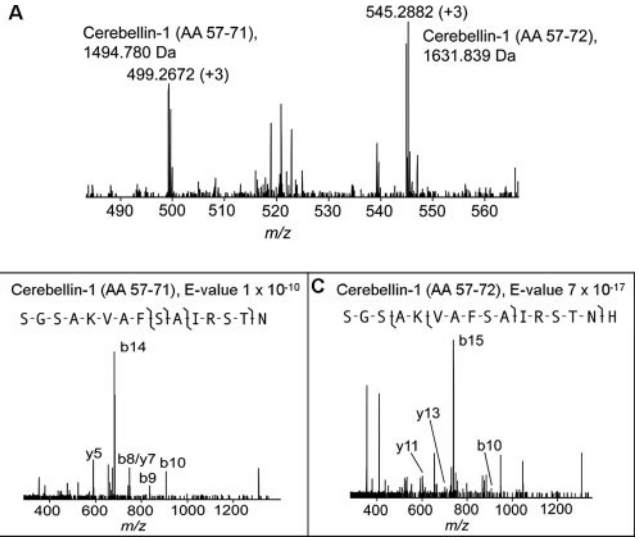

FIG. 2. **Identification of co-eluted truncated cerebellin and cerebellin.** The two peptides derived from cerebellin-1 precursor were detected in the same FTMS scan (*A*) and fragmented by a data-dependent MS/MS acquisition strategy and identified as SGSAKVAFSAIRSTN (*B*) and SGSAKVAFSAIRSTNH (*C*), respectively.

there was no report localizing these peptides to the SCN. Interestingly, our previous work on peptide release from the rat SCN demonstrated that an unknown peak at *m/z* 1495.75 (MH^+) changed in abundance with circadian rhythmicity over a 24-h period (30). Here, we confirm that this released peptide corresponds to a shortened form of cerebellin identified here with a 1×10^{-10} E-value.

Of the 102 SCN peptides identified, 12 harbored PTMs. One example is depicted in Fig. 3, showing FTMS and MS/MS spectra for two forms of manserin, which is derived from secretogranin 2 precursor. Manserin and phosphorylated manserin were identified with E-values of 6×10^{-50} and 4×10^{-23}, respectively, and the integrated intensity values of the peptides were similar at $\sim 5 \times 10^6$ and 1×10^6, respectively. Phosphorylated manserin exhibited the fragment ion generated by neutral loss of H_3PO_4 as the most prominent signal along with a few fragment ions of low abundance generated by fragmentation of the peptide backbone, which is a typical fragmentation pattern of Ser(P)/Thr(P) phosphopeptides.

Finally, Fig. 4 represents a search result using multiplexed MS/MS, which resulted from use of high resolution MS/MS data and our tailored software. In Fig. 4*A*, the isolation of a 5 *m/z* region for *m/z* 875.79 in the FTMS scan generates two isotopic distributions, which are 1744.964 and 2623.345 Da. In the data processing of ProSightPC, the two masses were searched independently using the entire fragment ion list derived from the Fig. 4*B* MS/MS scan and produced the identifications of two peptides that were derived from Rhombex-40 and pro-SAAS precursors, respectively, as seen in Fig. 4*C*. Rhombex-40 is known as a surface adhesion

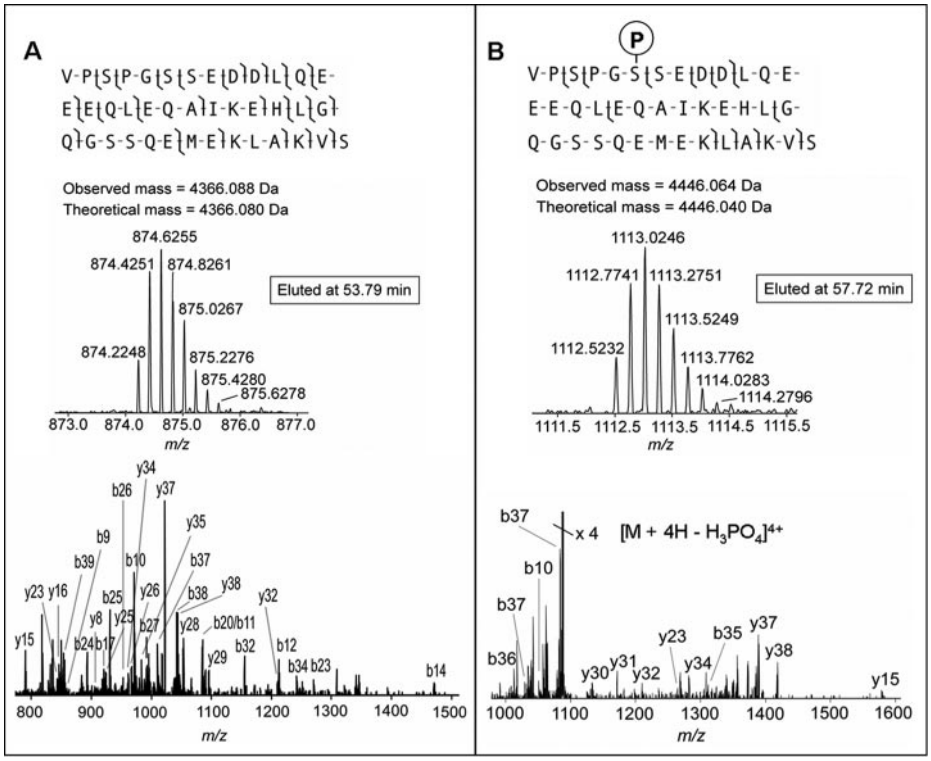

FIG. 3. **Identification of manserin with E-value of 6 × 10^{-50} (*A*) and phosphorylated manserin with E-value of 4 × 10^{-23} (*B*) by tailored software, ProSightPC.** The FTMS/MS spectrum of phosphorylated manserin exhibited the fragment ion generated by neutral loss of H_3PO_4 as the most prominent signal, which is a typical fragmentation pattern of Ser(P)/Thr(P) phosphopeptides by CID.

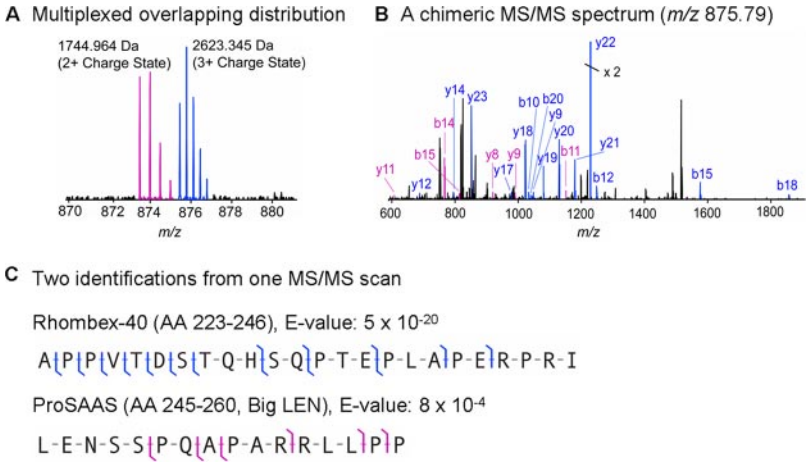

FIG. 4. **Multiplexed identification from high resolution FTMS/MS mass spectrum.** The two isotopic distributions corresponding to 1744.964 and 2623.345 Da (*A*) are seen in the isolation window for *m/z* 875.79 and generate the chimeric FTMS/MS spectrum (*B*). The tailored software, ProSightPC, produces the two peptides derived from Rhombex-40 and pro-SAAS precursors, respectively (*C*).

protein located at the ventral medullary surface (60); there is as yet no report of its expression in hypothalamus. The peptide big LEN, which is derived from pro-SAAS, was identified in our previous SCN studies (30).

DISCUSSION

Given that the SCN contains endogenous cellular oscillators that control the circadian rhythms of mammals, studying the peptides contained within the SCN is expected to increase our understanding of the circadian mechanisms. With solid-phase extraction collection strategies, we have recently analyzed the secreted peptides from the site of the SCN over a 24-h period and the released peptides from the SCN stimulated via the optic tract (30). We were able to identify several peptides previously reported by indirect studies to be present in the SCN. Furthermore, we discovered four new peptides, three of which are derived from pro-SAAS. One of the pro-SAAS-derived peptides, known as little SAAS, caused phase delays of SCN circadian rhythms *in vitro*.

However, there have not yet been any comprehensive peptidome studies of the SCN region using MS. Here, we performed the peptidome analysis of the rat hypothalamic SCN,

which was prepared during daytime (at ZT 6), and identified 102 endogenous peptides by FTMS/MS, including 33 novel peptides. Although most of the peptides, including the novel peptides, are produced from the cleavage of classical dibasic or monobasic neuropeptide processing sites, a number of peptides have cleavage sites at Leu-Ala or Leu-Leu, which could be products of Leu-*X*-specific enzyme (61). There were also several peptides with unconventional cleavage sites among the newly identified peptides, for example N-terminal or C-terminal side cleavage of aspartic acid (10, 61) of the peptides from pro-SAAS and C-terminal side cleavage of tryptophan of the peptide derived from neuropeptide Y. These cleavages could occur intracellularly during prohormone processing. Alternatively, these may be occurring during extracellular processing, either endogenously or perhaps during the preparation of tissue extracts. Physiological assessments, such as we have done for little SAAS (30), are necessary to determine the functional role(s) for our novel discovery products.

Many of the identified peptides in the present study were derived from known precursors expressed in the SCN. VIP (AA 125–152), GRP (AA 24–52), and somatostatin (AA 103–116) have been identified immunologically in neurons of the SCN core region. VIP and GRP have established roles in synchronization of the multitude of cell-based clocks in the SCN and also in relay of light information within the SCN to generate phase resetting of SCN tissue (25, 38–41, 48–50). In the present study, we observed shorter peptides derived from the VIP prohormone (AA 125–137) and GRP (AA 24–41) and the other peptide fragment of somatostatin (AA 25–87). The shortened forms of VIP and GRP have been observed in mice and reported in SwePep, whereas somatostatin (AA 103–116) has not been reported. As we stated above, these shortened forms may be from processing within the vesicle or may be from extracellular peptide processing; however, the possibility of degradation during our sample processing cannot be excluded. The reasons for not detecting several expected full-length peptides may be due to short peptide lifetimes, rapid degradation, or detection limits of FTMS/MS. Of course, the prior studies involving the localization of these peptides have used immunohistochemistry and so would not distinguish the full-length and shorter peptide forms. Thus, the unusual shortened forms of these well known peptides appear to be interesting targets for follow-up functional studies. Additionally, arginine-vasopressin (AVP), well known to be released and expressed at the shell neurons of the SCN (62), was identified with the loss of its C-terminal glycine to become an amidated peptide.

In addition to the forms of known intrinsic peptides of the SCN, a PACAP-related peptide, PACAP (AA 111–128) (10, 63), was identified in the present study, whereas the expected and well characterized PACAP peptides include those from AA 131–157 and 131–168. PACAP is known to be synthesized in the retina and released onto the SCN upon stimulation, transmitting photic signals via the retinohypothalamic tract (64–76). The observation of the unique peptide in the present study could indicate that the AA 111–128 fragment has some functional role, that PACAP is synthesized in the SCN, or that there is local translation of PACAP mRNA into its prohormone.

Neuropeptide Y and γ-aminobutyric acid (GABA) are putative transmitters of non-photic signals via the geniculohypothalamic tract to the SCN (77–91). We observed C-flanking peptide of neuropeptide Y, which was reported in geniculohypothalamic tract projections to the SCN (82), and the peptide fragment of GABA receptor subunit α-6. Although we identified three peptides derived from pro-SAAS in our previous releasate study of the SCN (30), here we were able to identify 18 peptides from pro-SAAS, including little SAAS, big SAAS, PEN, PEN-20, and big LEN.

In the present study, we also found multiple peptides that have not been previously reported in SCN circadian studies. CART, cerebellin-1, neuroendocrine protein 7B2, proenkephalin B, secretogranin 1, secretogranin 3, tachykinin 3, acyl-CoA-binding protein, brain-specific polypeptide PEP-19, PEBP-1, and dihydropyrimidinase-related proteins 2 and 3 (DRP-2 and DRP-3) precursors have not been reported in the prior SCN studies. Specifically, DRP-2 and DRP-3 are known to be expressed during neuronal ontogenesis and involve regulation of axon extension (92, 93) and have not been studied in the hypothalamus. Although the peptides derived from these precursors could have functional roles, the functional studies of the peptides are beyond the scope of our study.

Our current peptidome analysis by use of high resolution data and tailored software allowed the full characterization of 12 peptides with PTMs. The phosphorylated manserin (VPSPGS*(phosphorylation)SEDDLQEEEQLEQAIKEHLGQG-SSQEMEKLAKVS) derived from secretogranin 2 precursor was identified along with unmodified manserin. Secretogranin 2 is highly expressed in the SCN of mouse (94); however, no endogenous peptides derived from secretogranin 2 have been reported in SCN studies. Recently, Beranova-Giorgianni *et al.* (95) performed a phosphoproteomics analysis of the human pituitary sample with trypsin digestion followed by IMAC to enrich the phosphopeptides. They observed the phosphopeptide of SPGS(*)S(*)EDDLQEEEQLEQAIK; however, they were unable to determine which Ser site was phosphorylated between the two Ser sites denoted as (*) from their study. We also detected C-terminal amidation forms of neuropeptide-glutamic acid-isoleucine, neurosecretory protein VGF precursor (LEGSFLGGSEAGERLLQQGLAQVEA-NH_2), melanotropin α, substance P, AVP, and provasopressin (FQNCPRG-NH_2; truncated form of AVP). Specifically, the truncated form of AVP appears not to have been reported in prior studies. An AVP fragment produced from proteolysis in the brain has been reported to be a highly potent neuropeptide (96). In addition, we identified a pyroglutamylated form of secretogranin 1 precursor (Q(pyroglutamylation)YDDGVAELDQLLHY). Al-

though there is no report of this form of peptide in prior SCN studies, the homologous peptide was identified in bovine tissue adrenomedullary chromaffin vesicles (97).

In addition to peptides derived from prohormones, several peptides from non-prohormone-related proteins were detected, specifically four N-terminal acetylated forms of acyl-CoA-binding protein, brain-specific polypeptide PEP-19, thymosin β-4, and thymosin β-10. Many of these protein fragments have been reported in prior peptidome studies, and several, such as the thymosins, have been detected in SCN releasates (30), indicating that these proteins are endogenously processed into these shortened forms and may have some functional significance. Of course, others may represent sample preparation artifacts as the proteins may be degraded during tissue homogenization.

CONCLUSIONS

For identification and characterization of neuropeptides, the overall work flow described here represents a new route to discovery. Using MS/MS data with $\ll$10-ppm mass accuracy and neuroProSight software, higher quality identification is achieved. This information allows unusual PTMs to be confirmed. The overall sensitivity of the work flow allows such assays to be made on the small nuclei in the brain. Of course, additional developments will streamline this peptide discovery process.

From a neuroscience perspective, what is particularly exciting is combining peptide discovery with approaches optimized to measure peptide release (30, 98–101). The latter approaches provide a functional context for the peptide diversity determined here by allowing the subset of SCN peptides that are released at a particular time of day or under specific stimulation protocols to be uncovered. It is through the combination of peptide discovery and release assays that the functional implications on the complex interplay of a surprising range of peptides can be understood within the SCN.

Although we focused on analyzing the endogenous peptides present in SCN prepared at ZT 6 in the current study, the peptidome study at different ZTs can be considered as an important next step for better understanding how the SCN orchestrates circadian rhythms over a 24-h period. The SCN peptidome study at different ZTs including quantitative analysis of peptide expression is currently in progress.

Acknowledgments—We thank Dr. Andrew J. Forbes and Adrianna Bora for helpful discussions on data analysis and the sample processing protocol, respectively.

* This work was supported, in whole or in part, by National Institutes of Health Grant GM 067193-07 (to the laboratory of N. L. K.), Award DE018866 from the NIDCR and the Office of the Director (to J. V. S.), Grant HL092571 from the NHLBI (to M. U. G.), and Award DA018310 from the National Institute on Drug Abuse. This work was also supported by the Packard Foundation and the Sloan Foundation (to the laboratory of N. L. K.).

S The on-line version of this article (available at http://www.mcponline.org) contains supplemental Fig. S1 and Table 1.

‡‡ To whom correspondence should be addressed. E-mail: kelleher@scs.uiuc.edu.

REFERENCES

1. Strand, F. L. (1999) *Neuropeptides: Regulators of Physiological Processes*, The MIT Press, Cambridge, MA
2. Kandel E. R., Schwartz, J. H., and Jessell, T. M. (2000) *Principles of Neural Science*, 4th Ed., McGraw-Hill, New York
3. Burbach, J. P. H., and de Wied, D. (eds) (1993) *Brain Functions of Neuropeptides: a Current View*, Informa HealthCare, London
4. Hökfelt, T., Broberger, C., Xu, Z. Q., Sergeyev, V., Ubink, R., and Diez, M. (2000) Neuropeptides—an overview. *Neuropharmacology* **39,** 1337–1356
5. Hummon, A. B., Amare, A., and Sweedler, J. V. (2006) Discovering new invertebrate neuropeptides using mass spectrometry. *Mass Spectrom. Rev.* **25,** 77–98
6. Rossbach, U., Nilsson, A., Fälth, M., Kultima, K., Zhou, Q., Hallberg, M., Gordh, T., Andren, P. E., and Nyberg, F. (2009) A quantitative peptidomic analysis of peptides related to the endogenous opioid and tachykinin systems in nucleus accumbens of rats following naloxone-precipitated morphine withdrawal. *J. Proteome Res.* **8,** 1091–1098
7. Li, L., and Sweedler, J. V. (2008) Peptides in the brain: mass spectrometry-based measurement approaches and challenges. *Annu. Rev. Anal. Chem.* **1,** 451–483
8. Che, F. Y., Zhang, X., Berezniuk, I., Callaway, M., Lim, J., and Fricker, L. D. (2007) Optimization of neuropeptide extraction from the mouse hypothalamus. *J. Proteome Res.* **6,** 4667–4676
9. Fricker, L. D., Lim, J., Pan, H., and Che, F. Y. (2006) Peptidomics: Identification and quantification of endogenous peptides in neuroendocrine tissues. *Mass Spectrom. Rev.* **25,** 327–344
10. Dowell, J. A., Heyden, W. V., and Li, L. (2006) Rat neuropeptidomics by LC-MS/MS and MALDI-FTMS: enhanced dissection and extraction techniques coupled with 2D RP-RP HPLC. *J. Proteome Res.* **5,** 3368–3375
11. Fälth, M., Sköld, K., Svensson, M., Nilsson, A., Fenyö, D., and Andren, P. E. (2007) Neuropeptidomics strategies for specific and sensitive identification of endogenous peptides. *Mol. Cell. Proteomics* **6,** 1188–1197
12. Svensson, M., Sköld, K., Svenningsson, P., and Andren, P. E. (2003) Peptidomics-based discovery of novel neuropeptides. *J. Proteome Res.* **2,** 213–219
13. Taylor, S. W., Andon, N. L., Bilakovics, J. M., Lowe, C., Hanley, M. R., Pittner, R., and Ghosh, S. S. (2006) Efficient high-throughput discovery of large peptidic hormones and biomarkers. *J. Proteome Res.* **5,** 1776–1784
14. Ramström, M., Hagman, C., Tsybin, Y. O., Markides, K. E., Håkansson, P., Salehi, A., Lundquist, I., Håkanson, R., and Bergquist, J. (2003) A novel mass spectrometric approach to the analysis of hormonal peptides in extracts of mouse pancreatic islets. *Eur. J. Biochem.* **270,** 3146–3152
15. Wang, J., Ma, M., Chen, R., and Li, L. (2008) Enhanced neuropeptide profiling via capillary electrophoresis off-line coupled with MALDI FTMS. *Anal. Chem.* **80,** 6168–6177
16. Boyne, M. T., Garcia, B. A., Li, M., Zamdborg, L., Wenger, C. D., Babai, S., and Kelleher, N. L. (2009) Tandem mass spectrometry with ultrahigh mass accuracy clarifies peptide identification by database retrieval. *J. Proteome Res.* **8,** 374–379
17. Abrahamson, E. E., and Moore, R. Y. (2001) Suprachiasmatic nucleus in the mouse: retinal innervation, intrinsic organization and efferent projections. *Brain Res.* **916,** 172–191
18. Gillette, M. U., and Mitchell, J. W. (2002) Signaling in the suprachiasmatic nucleus: selectively responsive and integrative. *Cell Tissue Res.* **309,** 99–107
19. Leak, R. K., and Moore, R. Y. (2001) Topographic organization of suprachiasmatic nucleus projection neurons. *J. Comp. Neurol.* **433,** 312–334
20. Moore, R. Y., Speh, J. C., and Leak, R. K. (2002) Suprachiasmatic nucleus organization. *Cell Tissue Res.* **309,** 89–98
21. Morin, L. P., Shivers, K. Y., Blanchard, J. H., and Muscat, L. (2006) Complex organization of mouse and rat suprachiasmatic nucleus. *Neuroscience* **137,** 1285–1297

22. van den Pol, A. N., and Tsujimoto, K. L. (1985) Neurotransmitters of the hypothalamic suprachiasmatic nucleus immunocytochemical analysis of 25 neuronal antigens. *Neuroscience* **15,** 1049–1086
23. Karatsoreos, I. N., Yan, L., LeSauter, J., and Silver, R. (2004) Phenotype matters: Identification of light-responsive cells in the mouse suprachiasmatic nucleus. *J. Neurosci.* **24,** 68–75
24. van den Pol, A. N., Decavel, C., Levi, A., and Paterson, B. (1989) Hypothalamic expression of a novel gene product VGF immunocytochemical analysis. *J. Neurosci.* **9,** 4122–4137
25. van den Pol, A. N., and Gorcs, T. (1986) Synaptic relationships between neurons containing vasopressin gastrin-releasing peptide vasoactive intestinal polypeptide and glutamate decarboxylase immunoreactivity in the suprachiasmatic nucleus dual ultrastructural immunocytochemistry with gold-substituted silver peroxidase. *J. Comp. Neurol.* **252,** 507–521
26. Yan, L., Karatsoreos, I., Lesauter, J., Welsh, D. K., Kay, S., Foley, D., and Silver, R. (2007) Exploring spatiotemporal organization of SCN circuits. *Cold Spring Harb. Symp. Quant. Biol.* **72,** 527–541
27. Card, J. P., and Moore, R. Y. (1984) The suprachiasmatic nucleus of the golden-hamster: immunohistochemical analysis of cell and fiber distribution. *Neuroscience* **13,** 415–431
28. Morin, L. P. (2007) SCN organization reconsidered. *J. Biol. Rhythms* **22,** 3–13
29. van Leeuwen, F. W., Swaab, D. F., and de Raay, C. (1978) Immunoelectron microscopic localization of vasopressin in rat suprachiasmatic nucleus. *Cell Tissue Res.* **193,** 1–10
30. Hatcher, N. G., Atkins, N., Jr., Annangudi, S. P., Forbes, A. J., Kelleher, N. L., Gillette, M. U., and Sweedler, J. V. (2008) Mass spectrometry-based discovery of circadian peptides. *Proc. Natl. Acad. Sci. U.S.A.* **105,** 12527–12532
31. Leduc, R. D., and Kelleher, N. L. (2007) Using ProSight PTM and related tools for targeted protein identification and characterization with high mass accuracy tandem MS data. *Curr. Protoc. Bioinformatics* Chapter 13, 13.6.1–13.6.28
32. Zamdborg, L., LeDuc, R. D., Glowacz, K. J., Kim, Y. B., Viswanathan, V., Spaulding, I. T., Early, B. P., Bluhm, E. J., Babai, S., and Kelleher, N. L. (2007) ProSight PTM 2.0: improved protein identification and characterization for top down mass spectrometry. *Nucleic Acids Res.* **35,** W701–W706
33. Bora, A., Annangudi, S. P., Millet, L. J., Rubakhin, S. S., Forbes, A. J., Kelleher, N. L., Gillette, M. U., and Sweedler, J. V. (2008) Neuropeptidomics of the supraoptic rat nucleus. *J. Proteome Res.* **7,** 4992–5003
34. Tischkau, S. A., Mitchell, J. W., Pace, L. A., Barnes, J. W., Barnes, J. A., and Gillette, M. U. (2004) Protein kinase G type II is required for night-to-day progression of the mammalian circadian clock. *Neuron* **43,** 539–549
35. Southey, B. R., Amare, A., Zimmerman, T. A., Rodriguez-Zas, S. L., and Sweedler, J. V. (2006) NeuroPred: a tool to predict cleavage sites in neuropeptide precursors and provide the masses of the resulting peptides. *Nucleic Acids Res.* **34,** W267–W272
36. Amare, A., Hummon, A. B., Southey, B. R., Zimmerman, T. A., Rodriguez-Zas, S. L., and Sweedler, J. V. (2006) Bridging neuropeptidomics and genomics with bioinformatics: prediction of mammalian neuropeptide prohormone processing. *J. Proteome Res.* **5,** 1162–1167
37. Tegge, A. N., Southey, B. R., Sweedler, J. V., and Rodriguez-Zas, S. L. (2008) Comparative analysis of neuropeptide cleavage sites in human, mouse, rat, and cattle. *Mamm. Genome* **19,** 106–120
38. Albers, H. E., Gillespie, C. F., Babagbemi, T. O., and Huhman, K. L. (1995) Analysis of the phase-shifting effects of gastrin-releasing peptide when microinjected into the suprachiasmatic region. *Neurosci. Lett.* **191,** 63–66
39. Brown, T. M., Hughes, A. T., and Piggins, H. D. (2005) Gastrin-releasing peptide promotes suprachiasmatic nuclei cellular rhythmicity in the absence of vasoactive intestinal polypeptide-VPAC(2) receptor signaling. *J. Neurosci.* **25,** 11155–11164
40. Gamble, K. L., Allen, G. C., Zhou, T., and McMahon, D. G. (2007) Gastrin-releasing peptide mediates light-like resetting of the suprachiasmatic nucleus circadian pacemaker through cAMP response element-binding protein and Per1 activation. *J. Neurosci.* **27,** 12078–12087
41. McArthur, A. J., Coogan, A. N., Ajpru, S., Sugden, D., Biello, S. M., and Piggins, H. D. (2000) Gastrin-releasing peptide phase-shifts suprachiasmatic nuclei neuronal rhythms in vitro. *J. Neurosci.* **20,** 5496–5502
42. Aida, R., Moriya, T., Araki, M., Akiyama, M., Wada, K., Wada, E., and Shibata, S. (2002) Gastrin-releasing peptide mediates photic entrainable signals to dorsal subsets of suprachiasmatic nucleus via induction of Period gene in mice. *Mol. Pharmacol.* **61,** 26–34
43. Aïoun, J., Chambille, I., Peytevin, J., and Martinet, L. (1998) Neurons containing gastrin-releasing peptide and vasoactive intestinal polypeptide are involved in the reception of the photic signal in the suprachiasmatic nucleus of the Syrian hamster: an immunocytochemical ultrastructural study. *Cell Tissue Res.* 2**91,** 239–253
44. Antle, M. C., Kriegsfeld, L. J., and Silver, R. (2005) Signaling within the master clock of the brain: Localized activation of mitogen-activated protein kinase by gastrin-releasing peptide. *J. Neurosci.* **25,** 2447–2454
45. Earnest, D. J., DiGiorgio, S., and Olschowka, J. A. (1993) Light induces expression of Fos-related proteins within gastrin-releasing peptide neurons in the rat suprachiasmatic nucleus. *Brain Res.* **627,** 205–209
46. Kallingal, G. J., and Mintz, E. M. (2006) Glutamatergic activity modulates the phase-shifting effects of gastrin-releasing peptide and light. *Eur. J. Neurosci.* **24,** 2853–2858
47. Piggins, H. D., Goguen, D., and Rusak, B. (2005) Gastrin-releasing peptide induces c-Fos in the hamster suprachiasmatic nucleus. *Neurosci. Lett.* **384,** 205–210
48. Aton, S. J., Colwell, C. S., Harmar, A. J., Waschek, J., and Herzog, E. D. (2005) Vasoactive intestinal polypeptide mediates circadian rhythmicity and synchrony in mammalian clock neurons. *Nat. Neurosci.* **8,** 476–483
49. Piggins, H. D., and Cutler, D. J. (2003) The roles of vasoactive intestinal polypeptide in the mammalian circadian clock. *J. Endocrinol.* **177,** 7–15
50. Vosko, A. M., Schroeder, A., Loh, D. H., and Colwell, C. S. (2007) Vasoactive intestinal peptide and the mammalian circadian system. *Gen. Comp. Endocrinol.* **152,** 165–175
51. Card, J. P., Brecha, N., Karten, H. J., and Moore, R. Y. (1981) Immunocytochemical localization of vasoactive intestinal polypeptide-containing cells and processes in the suprachiasmatic nucleus of the rat: light and electron-microscopic analysis. *J. Neurosci.* **1,** 1289–1303
52. Colwell, C. S., Michel, S., Itri, J., Rodriguez, W., Tam, J., Lelievre, V., Hu, Z., Liu, X., and Waschek, J. A. (2003) Disrupted circadian rhythms in VIP- and PHI-deficient mice. *Am. J. Physiol. Regul. Integr. Comp. Physiol.* **285,** R939–R949
53. Hannibal, J., and Fahrenkrug, J. (2003) Circadian rhythm regulation: a central role for the neuropeptide vasoactive intestinal polypeptide. *Am. J. Physiol. Regul. Integr. Comp. Physiol.* **285,** R935–R936
54. Kawamoto, K., Nagano, M., Kanda, F., Chihara, K., Shigeyoshi, Y., and Okamura, H. (2003) Two types of VIP neuronal components in rat suprachiasmatic nucleus. *J. Neurosci. Res.* **74,** 852–857
55. Sims, K. B., Hoffman, D. L., Said, S. I., and Zimmerman, E. A. (1980) Vasoactive intestinal polypeptide (VIP) in mouse and rat brain: an immunocytochemical study. *Brain Res.* **186,** 165–183
56. Lein, E. S., Hawrylycz, M. J., Ao, N., Ayres, M., Bensinger, A., Bernard, A., Boe, A. F., Boguski, M. S., Brockway, K. S., Byrnes, E. J., Chen, L., Chen, L., Chen, T. M., Chin, M. C., Chong, J., Crook, B. E., Czaplinska, A., Dang, C. N., Datta, S., Dee, N. R., Desaki, A. L., Desta, T., Diep, E., Dolbeare, T. A., Donelan, M. J., Dong, H. W., Dougherty, J. G., Duncan, B. J., Ebbert, A. J., Eichele, G., Estin, L. K., Faber, C., Facer, B. A., Fields, R., Fischer, S. R., Fliss, T. P., Frensley, C., Gates, S. N., Glattfelder, K. J., Halverson, K. R., Hart, M. R., Hohmann, J. G., Howell, M. P., Jeung, D. P., Johnson, R. A., Karr, P. T., Kawal, R., Kidney, J. M., Knapik, R. H., Kuan, C. L., Lake, J. H., Laramee, A. R., Larsen, K. D., Lau, C., Lemon, T. A., Liang, A. J., Liu, Y., Luong, L. T., Michaels, J., Morgan, J. J., Morgan, R. J., Mortrud, M. T., Mosqueda, N. F., Ng, L. L., Ng, R., Orta, G. J., Overly, C. C., Pak, T. H., Parry, S. E., Pathak, S. D., Pearson, O. C., Puchalski, R. B., Riley, Z. L., Rockett, H. R., Rowland, S. A., Royall, J. J., Ruiz, M. J., Sarno, N. R., Schaffnit, K., Shapovalova, N. V., Sivisay, T., Slaughterbeck, C. R., Smith, S. C., Smith, K. A., Smith, B. I., Sodt, A. J., Stewart, N. N., Stumpf, K. R., Sunkin, S. M., Sutram, M., Tam, A., Teemer, C. D., Thaller, C., Thompson, C. L., Varnam, L. R., Visel, A., Whitlock, R. M., Wohnoutka, P. E., Wolkey, C. K., Wong, V. Y., Wood, M., Yaylaoglu, M. B., Young, R. C., Youngstrom, B. L., Yuan, X. F., Zhang, B., Zwingman, T. A., and Jones, A. R. (2007) Genome-wide atlas of gene expression in the adult mouse brain. *Nature* **445,** 168–176
57. Lippton, H., Lin, B., Gumusel, B., Witriol, N., Wasserman, A., and Knight, M. (2006) Hemopressin, a hemoglobin fragment, dilates the rat systemic vascular bed through release of nitric oxide. *Peptides* **27,** 2284–2288

58. Heimann, A. S., Gomes, I., Dale, C. S., Pagano, R. L., Gupta, A., de Souza, L. L., Luchessi, A. D., Castro, L. M., Giorgi, R., Rioli, V., Ferro, E. S., and Devi, L. A. (2007) Hemopressin is an inverse agonist of CB1 cannabinoid receptors. *Proc. Natl. Acad. Sci. U.S.A.* **104,** 20588–20593
59. Nydahl, K. S., Pierson, J., Nyberg, F., Caprioli, R. M., and Andrén, P. E. (2003) In vivo processing of LVV-hemorphin-7 in rat brain and blood utilizing microdialysis combined with electrospray mass spectrometry. *Rapid Commun. Mass Spectrom.* **17,** 838–844
60. Shimokawa, N., Jingu, H., Okada, J., and Miura, M. (2000) Molecular cloning of Rhombex-40 a transmembrane protein from the ventral medullary surface of the rat brain by differential display. *Life Sci.* **66,** 2183–2191
61. Che, F. Y., Lim, J., Pan, H., Biswas, R., and Fricker, L. D. (2005) Quantitative neuropeptidomics of microwave-irradiated mouse brain and pituitary. *Mol. Cell. Proteomics* **4,** 1391–1405
62. Gillette, M. U., and Reppert, S. M. (1987) The hypothalamic suprachiasmatic nuclei: circadian patterns of vasopressin secretion and neuronal activity in vitro. *Brain Res. Bull.* **19,** 135–139
63. Faith, M., Skold, K., Svensson, M., Norrman, M., Nilsson, A., Fenyo, D., and Andren, P. (2006) SWEPEP, a database designed for neuropeptides and mass spectrometry. *Mol. Cell. Proteomics* **5,** 998–1005
64. Butcher, G. Q., Lee, B., Cheng, H. Y., and Obrietan, K. (2005) Light stimulates MSK1 activation in the suprachiasmatic nucleus via a PACAP-ERK/MAP kinase-dependent mechanism. *J. Neurosci.* **25,** 5305–5313
65. Chen, D., Buchanan, G. F., Ding, J. M., Hannibal, J., and Gillette, M. U. (1999) Pituitary adenylyl cyclase-activating peptide: a pivotal modulator of glutamatergic regulation of the suprachiasmatic circadian clock. *Proc. Natl. Acad. Sci. U.S.A.* **96,** 13468–13473
66. Dziema, H., and Obrietan, K. (2002) PACAP potentiates L-type calcium channel conductance in suprachiasmatic nucleus neurons by activating the MAPK pathway. *J. Neurophysiol.* **88,** 1374–1386
67. Hannibal, J. (2002) Neurotransmitters of the retino-hypothalamic tract. *Cell Tissue Res.* **309,** 73–88
68. Hannibal, J. (2006) Roles of PACAP-containing retinal ganglion cells in circadian timing. *Int. Rev. Cytol.* **251,** 1–39
69. Hannibal, J., Ding, J. M., Chen, D., Fahrenkrug, J., Larsen, P. J., Gillette, M. U., and Mikkelsen, J. D. (1998) Pituitary adenylate cyclase activating peptide (PACAP) in the retinohypothalamic tract: a daytime regulator of the biological clock. *Ann. N.Y. Acad. Sci.* **865,** 197–206
70. Hannibal, J., Ding, J. M., Chen, D., Fahrenkrug, J., Larsen, P. J., Gillette, M. U., and Mikkelsen, J. D. (1997) Pituitary adenylate cyclase-activating peptide (PACAP) in the retinohypothalamic tract: a potential daytime regulator of the biological clock. *J. Neurosci.* **17,** 2637–2644
71. Hannibal, J., and Fahrenkrug, J. (2004) Target areas innervated by PACAP-immunoreactive retinal ganglion cells. *Cell Tissue Res.* **316,** 99–113
72. Hannibal, J., Hindersson, P., Ostergaard, J., Georg, B., Heegaard, S., Larsen, P. J., and Fahrenkrug, J. (2004) Melanopsin is expressed in PACAP-containing retinal ganglion cells of the human retinohypothalamic tract. *Invest. Ophthalmol. Vis. Sci.* **45,** 4202–4209
73. Kopp, M. D., Meissl, H., Dehghani, F., and Korf, H. W. (2001) The pituitary adenylate cyclase-activating polypeptide modulates glutamatergic calcium signalling: investigations on rat suprachiasmatic nucleus neurons. *J. Neurochem.* **79,** 161–171
74. Kopp, M. D., Schomerus, C., Dehghani, F., Korf, H. W., and Meissl, H. (1999) Pituitary adenylate cyclase-activating polypeptide and melatonin in the suprachiasmatic nucleus: effects on the calcium signal transduction cascade. *J. Neurosci.* **19,** 206–219
75. Minami, Y., Furuno, K., Akiyama, M., Moriya, T., and Shibata, S. (2002) Pituitary adenylate cyclase-activating polypeptide produces a phase shift associated with induction of mPer expression in the mouse suprachiasmatic nucleus. *Neuroscience* **113,** 37–45
76. Beaulé, C., Mitchell, J. W., Lindberg, P. T., Damadzic, R., Eiden, L. E., and Gillette, M. U. (2009) Temporally restricted role of retinal PACAP: integration of the phase-advancing light signal to the SCN. *J. Biol. Rhythms* **24,** 126–134
77. Medanic, M., and Gillette, M. U. (1993) Suprachiasmatic circadian pacemaker of rat shows 2 windows of sensitivity to neuropeptide Y in vitro. *Brain Res.* **620,** 281–286
78. Albers, H. E., and Ferris, C. F. (1984) Neuropeptide Y role in light-dark cycle entrainment of hamster circadian rhythms. *Neurosci. Lett.* **50,** 163–168
79. Biello, S. M., and Mrosovsky, N. (1996) Phase response curves to neuropeptide Y in wildtype and tau mutant hamsters. *J. Biol. Rhythms* **11,** 27–34
80. Brewer, J. M., Yannielli, P. C., and Harrington, M. E. (2002) Neuropeptide Y differentially suppresses per1 and per2 mRNA induced by light in the suprachiasmatic nuclei of the golden hamster. *J. Biol. Rhythms* **17,** 28–39
81. Card, J. P., and Moore, R. Y. (1988) Neuropeptide Y localization in the rat suprachiasmatic nucleus and periventricular hypothalamus. *Neurosci. Lett.* **88,** 241–246
82. Card, J. P., and Moore, R. Y. (1989) Organization of lateral geniculate-hypothalamic connections in the rat. *J. Comp. Neurol.* **284,** 135–147
83. Fukuhara, C., Brewer, J. M., Dirden, J. C., Bittman, E. L., Tosini, G., and Harrington, M. E. (2001) Neuropeptide Y rapidly reduces Period 1 and Period 2 mRNA levels in the hamster suprachiasmatic nucleus. *Neurosci. Lett.* **314,** 119–122
84. Harrington, M. E., Nance, D. M., and Rusak, B. (1985) Neuropeptide-Y immunoreactivity in the hamster geniculo-suprachiasmatic tract. *Brain Res. Bull.* **15,** 465–472
85. Huhman, K. L., Gillespie, C. F., Marvel, C. L., and Albers, H. E. (1996) Neuropeptide Y phase shifts circadian rhythms in vivo via a Y-2 receptor. *Neuroreport* **7,** 1249–1252
86. Lall, G. S., and Biello, S. M. (2003) Attenuation of circadian light induced phase advances and delays by neuropeptide Y and a neuropeptide YY1/Y5 receptor agonist. *Neuroscience* **119,** 611–618
87. O'Hara, B. F., Andretic, R., Heller, H. C., Carter, D. B., and Kilduff, T. S. (1995) GABAA, GABAC, and NMDA receptor subunit expression in the suprachiasmatic nucleus and other brain regions. *Brain Res. Mol. Brain Res.* **28,** 239–250
88. Prosser, R. A. (1998) Neuropeptide Y blocks serotonergic phase shifts of the suprachiasmatic circadian clock in vitro. *Brain Res.* **808,** 31–41
89. van den Pol, A. N., Obrietan, K., Chen, G., and Belousov, A. B. (1996) Neuropeptide Y-mediated long-term depression of excitatory activity in suprachiasmatic nucleus neurons. *J. Neurosci.* **16,** 5883–5895
90. Weber, E. T., and Rea, M. A. (1997) Neuropeptide Y blocks light-induced phase advances but not delays of the circadian activity rhythm in hamsters. *Neurosci. Lett.* **231,** 159–162
91. Yannielli, P. C., Brewer, J. M., and Harrington, M. E. (2004) Blockade of the NPYY5 receptor potentiates circadian responses to light: complementary in vivo and in vitro studies. *Eur. J. Neurosci.* **19,** 891–897
92. Minturn, J. E., Fryer, H. J., Geschwind, D. H., and Hockfield, S. (1995) Toad-64, a gene expressed early in neuronal differentiation in the rat, is related to Unc-33, a C-Elegans gene involved in axon outgrowth. *J. Neurosci.* **15,** 6757–6766
93. Quinn, C. C., Chen, E., Kinjo, T. G., Kelly, G., Bell, A. W., Elliott, R. C., McPherson, P. S., and Hockfield, S. (2003) TUC-4b, a novel TUC family variant, regulates neurite outgrowth and associates with vesicles in the growth cone. *J. Neurosci.* **23,** 2815–2823
94. Hong, H. K., Chong, J. L., Song, W. M., Song, E. J., Jyawook, A. A., Schook, A. C., Ko, C. H., and Takahashi, J. S. (2007) Inducible and reversible clock gene expression in brain using the tTA system for the study of circadian behavior. *PLoS Genet.* **3,** 324–338
95. Beranova-Giorgianni, S., Zhao, Y., Desiderio, D. M., and Giorgianni, F. (2006) Phosphoproteomic analysis of the human pituitary. *Pituitary* **9,** 109–120
96. Burbach, J. P., Kovács, G. L., de Wied, D., van Nispen, J. W., and Greven, H. M. (1983) A major metabolite of arginine vasopressin in the brain is a highly potent neuropeptide. *Science* **221,** 1310–1312
97. Flanagan, T., Taylor, L., Poulter, L., Viveros, O. H., and Diliberto, E. J., Jr. (1990) A novel 1745-dalton pyroglutamyl peptide derived from chromogranin-B is in the bovine adrenomedullary chromaffin vesicle. *Cell. Mol. Neurobiol.* **10,** 507–523
98. Iannacone, J. M., Ren, S., Hatcher, N. G., and Sweedler, J. V. (2009) Collecting peptide release from the brain using porous polymer monolith-based solid phase extraction capillaries. *Anal. Chem.* **81,** 5433–5438
99. Hatcher, N. G., Richmond, T. A., Rubakhin, S. S., and Sweedler, J. V. (2005) Monitoring activity-dependent peptide release from the CNS using single-bead solid-phase extraction and MALDI TOF MS detection.

Anal. Chem. **77,** 1580–1587
100. Haskins, W. E., Watson, C. J., Cellar, N. A., Powell, D. H., and Kennedy, R. T. (2004) Discovery and neurochemical screening of peptides in brain extracellular fluid by chemical analysis of in vivo microdialysis samples. *Anal. Chem.* **76,** 5523–5533
101. Li, Q., Zubieta, J. K., and Kennedy, R. T. (2009) Practical aspects of in vivo detection of neuropeptides by microdialysis coupled off-line to capillary LC with multistage MS. *Anal. Chem.* **81,** 2242–2250
102. Zhang, X., Che, F. Y., Berezniuk, I., Sonmez, K., Toll, L., and Fricker, L. D. (2008) Peptidomics of Cpe(fat/fat) mouse brain regions: implications for neuropeptide processing. *J. Neurochem.* **107,** 1596–1613
103. Abrahamson, E. E., Leak, R. K., and Moore, R. Y. (2001) The suprachiasmatic nucleus projects to posterior hypothalamic arousal systems. *Neuroreport* **12,** 435–440
104. Levi, A., Ferri, G. L., Watson, E., Possenti, R., and Salton, S. R. (2004) Processing, distribution, and function of VGF, a neuronal and endocrine peptide precursor. *Cell. Mol. Neurobiol.* **24,** 517–533
105. Okamura, H., Tanaka, M., Kanemasa, K., Ban, Y., Inouye, S. I., and Ibata, Y. (1994) In situ hybridization histochemistry of Vghm1f messenger RNA in the rat suprachiasmatic nucleus: co-localization with vasopressin neurophysin and VIP-PHI. *Neurosci. Lett.* **182,** 181–184
106. Okamura, H., Tanaka, M., Kanemasa, K., Ban, Y., Inouye, S. I., and Ibata, Y. (1995) In situ hybridization histochemistry of VGF mRNA in the rat suprachiasmatic nucleus: co-localization with vasopressin/neurophysin and VIP/PHI. *Neurosci. Lett.* **189,** 181a–184a
107. Snyder, S. E., and Salton, S. R. (1998) Expression of VGF mRNA in the adult rat central nervous system. *J. Comp. Neurol.* **394,** 91–105
108. Wisor, J. P., and Takahashi, J. S. (1997) Regulation of the VGF gene in the golden hamster suprachiasmatic nucleus by light and by the circadian clock. *J. Comp. Neurol.* **378,** 229–238
109. Yamaguchi, H., Sasaki, K., Satomi, Y., Shimbara, T., Kageyama, H., Mondal, M. S., Toshinai, K., Date, Y., González, L. J., Shioda, S., Takao, T., Nakazato, M., and Minamino, N. (2007) Peptidomic identification and biological validation of neuroendocrine regulatory peptide-1 and -2. *J. Biol. Chem.* **282,** 26354–26360
110. Kopp, M., Meissl, H., and Korf, H. W. (1997) The pituitary adenylate cyclase-activating polypeptide-induced phosphorylation of the transcription factor CREB (cAMP response element binding protein) in the rat suprachiasmatic nucleus is inhibited by melatonin. *Neurosci. Lett.* **227,** 145–148
111. Kiss, J. Z., Cassell, M. D., and Palkovits, M. (1984) Analysis of the ACTH beta-end alpha-MSH-immunoreactive afferent input to the hypothalamic paraventricular nucleus of rat. *Brain Res.* **324,** 91–99
112. Barden, N., Mérand, Y., Rouleau, D., Garon, M., and Dupont, A. (1981) Changes in the beta-endorphin content of discrete hypothalamic nuclei during the estrous-cycle of the rat. *Brain Res.* **204,** 441–445
113. Tuinhof, R., Artero, C., Fasolo, A., Franzoni, M. F., Ten Donkelaar, H. J., Wismans, P. G., and Roubos, E. W. (1994) Involvement of retinohypothalamic input, suprachiasmatic nucleus, magnocellular nucleus and locus coeruleus in control of melanotrope cells of Xenopus laevis: a retrograde and anterograde tracing study. *Neuroscience* **61,** 411–420
114. Marani, E., Rietveld, W. J., Luiten, P. G., and van der Veeken, J. G. (1987) Cell typing and connections of the rat suprachiasmatic nucleus. *Prog. Clin. Biol. Res.* **227A,** 199–213
115. Zamir, N., Palkovits, M., and Brownstein, M. (1985) Distribution of immunoreactive Met-enkephalin-Arg6-Gly7-Leu8 and Leu-enkephalin in discrete regions of the rat brain. *Brain Res.* **326,** 1–8
116. Bernay, B., Gaillard, M. C., Guryca, V., Emadali, A., Kuhn, L., Bertrand, A., Detraz, I., Carcenac, C., Savasta, M., Brouillet, E., Garin, J., and Elalouf, J. M. (2009) Discovering new bioactive neuropeptides in the striatum secretome using in vivo microdialysis and versatile proteomics. *Mol. Cell. Proteomics* **8,** 946–958
117. Abe, H., Honma, S., Shinohara, K., and Honma, K. (1996) Substance P receptor regulates the photic induction of Fos-like protein in the suprachiasmatic nucleus of Syrian hamsters. *Brain Res.* **708,** 135–142
118. Hannibal, J., and Fahrenkrug, J. (2002) Immunoreactive substance P is not part of the retinohypothalamic tract in the rat. *Cell Tissue Res.* **309,** 293–299
119. Mikkelsen, J. D., and Larsen, P. J. (1993) Substance-P in the suprachiasmatic nucleus of the rat: an immunohistochemical and in-situ hybridization study. *Histochemistry* **100,** 3–16
120. Otori, Y., Tominaga, K., Fukuhara, C., Yang, J., Yamazaki, S., Cagampang, F. R., Okamura, H., and Inouye, S. T. (1993) Substance P-like immunoreactivity in the suprachiasmatic nucleus of the rat. *Brain Res.* **619,** 271–277
121. Piggins, H. D., and Rusak, B. (1997) Effects of microinjections of substance P into the suprachiasmatic nucleus region on hamster wheel-running rhythms. *Brain Res. Bull.* **42,** 451–455
122. Shibata, S., Tsuneyoshi, A., Hamada, T., Tominaga, K., and Watanabe, S. (1992) Effect of substance P on circadian-rhythms of firing activity and the 2-deoxyglucose uptake in the rat suprachiasmatic nucleus in vitro. *Brain Res.* **597,** 257–263
123. Shigeyoshi, Y., Maebayashi, Y., and Okamura, H. (1997) Co-localization of preprosomatostatin mRNA and preprotachykinin A mRNA in neurons of the rat suprachiasmatic nucleus. *Brain Res. Mol. Brain Res.* **48,** 159–163
124. Fricker, L. D., McKinzie, A. A., Sun, J., Curran, E., Qian, Y., Yan, L., Patterson, S. D., Courchesne, P. L., Richards, B., Levin, N., Mzhavia, N., Devi, L. A., and Douglass, J. (2000) Identification and characterization of proSAAS, a granin-like neuroendocrine peptide precursor that inhibits prohormone processing. *J. Neurosci.* **20,** 639–648
125. Gary, K. A., Sollars, P. J., Lexow, N., Winokur, A., and Pickard, G. E. (1996) Thyrotropin-releasing hormone phase shifts circadian rhythms in hamsters. *Neuroreport* **7,** 1631–1634
126. Lechan, R. M., and Jackson, I. M. D. (1982) Immunohistochemical localization of thyrotropin-releasing hormone in the rat hypothalamus and pituitary. *Endocrinology* **111,** 55–65
127. Parkin, M. C., Wei, H., O'Callaghan, J. P., and Kennedy, R. T. (2005) Sample-dependent effects on the neuropeptidome detected in rat brain tissue preparations by capillary liquid chromatography with tandem mass spectrometry. *Anal. Chem.* 7**7,** 6331–6338
128. Pan, H., Che, F. Y., Peng, B., Steiner, D. F., Pintar, J. E., and Fricker, L. D. (2006) The role of prohormone convertase-2 in hypothalamic neuropeptide processing: a quantitative neuropeptidomic study. *J. Neurochem.* **98,** 1763–1777
129. Biemans, B. A., Gerkema, M. P., and Van der Zee, E. A. (2002) Increase in somatostatin immunoreactivity in the suprachiasmatic nucleus of aged Wistar rats. *Brain Res.* **958,** 463–467
130. Fukuhara, C., Shinohara, K., Tominaga, K., Otori, Y., and Inouye, S. T. (1993) Endogenous circadian rhythmicity of somatostatin-like immunoreactivity in the rat suprachiasmatic nucleus. *Brain Res.* **606,** 28–35
131. Shinohara, K., Isobe, Y., Takeuchi, J., and Inouye, S. T. (1991) Circadian-rhythms of somatostatin-immunoreactivity in the suprachiasmatic nucleus of the rat. *Neurosci. Lett.* **129,** 59–62
132. Vandesande, F., Dierickx, K., and DeMey, J. (1975) Identification of vasopressin-neurophysin producing neurons of rat suprachiasmatic nuclei. *Cell Tissue Res.* **156,** 377–380
133. Che, F. Y., Yuan, Q., Kalinina, E., and Fricker, L. D. (2005) Pedtidomics of Cpe(fat/fat) mouse hypothalamus: effect of food deprivation and exercise on peptide levels. *J. Biol. Chem.* **280,** 4451–4461
134. Alho, H., Fremeau, R. T., Jr., Tiedge, H., Wilcox, J., Bovolin, P., Brosius, J., Roberts, J. L., and Costa, E. (1988) Diazepam binding inhibitor gene expression: location in brain and peripheral tissues of rat. *Proc. Natl. Acad. Sci. U.S.A.* **85,** 7018–7022
135. Guidotti, A., Toffano, G., and Costa, E. (1978) Endogenous protein modulates affinity of GABA and benzodiazepine receptors in rat brain. *Nature* **275,** 553–555
136. Ziai, R., Pan, Y. C., Hulmes, J. D., Sangameswaran, L., and Morgan, J. I. (1986) Isolation, sequence, and developmental profile of a brain-specific polypeptide, Pep-19. *Proc. Natl. Acad. Sci. U.S.A.* **83,** 8420–8423
137. Wei, H., Dean, S. L., Parkin, M. C., Nolkrantz, K., O'Callaghan, J. P., and Kennedy, R. T. (2005) Microscale sample deposition onto hydrophobic target plates for trace level detection of neuropeptides in brain tissue by MALDI-MS. *J. Mass Spectrom.* **40,** 1338–1346